KJPP

Original Article

Anti-cancer effects of fenbendazole on 5-fluorouracil-resistant colorectal cancer cells

Deokbae Park[1,#], Jung-Hee Lee[2,#], and Sang-Pil Yoon[3,*]

[1]Department of Histology, College of Medicine, Jeju National University, Jeju 63243, [2]Department of Cellular and Molecular Medicine, Chosun University School of Medicine, Gwangju 61452, [3]Department of Anatomy, College of Medicine, Jeju National University, Jeju 63243, Korea

ABSTRACT Benzimidazole anthelmintic agents have been recently repurposed to overcome cancers resistant to conventional therapies. To evaluate the anti-cancer effects of benzimidazole on resistant cells, various cell death pathways were investigated in 5-fluorouracil-resistant colorectal cancer cells. The viability of wild-type and 5-fluorouracil-resistant SNU-C5 colorectal cancer cells was assayed, followed by Western blotting. Flow cytometry assays for cell death and cell cycle was also performed to analyze the anti-cancer effects of benzimidazole. When compared with albendazole, fenbendazole showed higher susceptibility to 5-fluorouracil-resistant SNU-C5 cells and was used in subsequent experiments. Flow cytometry revealed that fenbendazole significantly induces apoptosis as well as cell cycle arrest at G2/M phase on both cells. When compared with wild-type SNU-C5 cells, 5-fluorouracil-resistant SNU-C5 cells showed reduced autophagy, increased ferroptosis and ferroptosis-augmented apoptosis, and less activation of caspase-8 and p53. These results suggest that fenbendazole may be a potential alternative treatment in 5-fluorouracil-resistant cancer cells, and the anticancer activity of fenbendazole does not require p53 in 5-fluorouracil-resistant SNU-C5 cells.

INTRODUCTION

Drug repositioning of approved therapies might extend their therapeutic potential against resistant cancer cells [1]. Benzimidazole anthelmintic agents are relatively non-toxic to normal cells [2-6] with a half-maximal inhibitory concentration (IC_{50}) of 5 μM for less sensitivity in 461 cancer cells [7]. A recent report summarized the anti-tumourigenic activity of benzimidazole as follows [1]: 1) cell cycle arrest at G2/M phase with increased levels of cyclin B1, p21 and p27Kip1; 2) apoptosis with increased expression of caspase-3, poly (ADP-ribose) polymerase (PARP), and cytochrome-C; 3) autophagy with increased microtubule-associated protein 1A/1B-light chain 3 (LC3) and Beclin-1; and 4) altered cell viability or differentiation with increased p53, p21, p38, and c-Jun N-terminal kinase (JNK), and decreased extracellular signal-regulated protein kinase (ERK).

Self-administration of fenbendazole, a benzimidazole anthelmintic agent, by patients with cancer has been reported in social media [8,9]. Although anti-cancer effects of fenbendazole as an alternative or supplementary agent were recently reported in a case series of genitourinary malignancies [10], no definitive evidence of anti-cancer effects exists in human because of its toxicity and teratogenicity [8]. Nevertheless, the potential for drug repositioning of fenbendazole requires further investigation because of the much higher IC_{50} values in normal cells compared with cancer cells [5].

Colorectal cancer (CRC) is the third most common cancer diagnosed and the second leading cause of cancer death worldwide [11]. Although 5-fluorouracil (5-FU) remains the mainstay of standard chemotherapy for CRC, various resistance mechanisms

are reported [12]. Especially, mutations in p53 [13-15] or p38α mitogen-activated protein kinase (MAPK) [16,17] are associated with chemo-resistant CRC. To overcome the resistance, activation of transforming growth factor-β [18] or ERK [19] was suggested in 5-FU-resistant CRC cell line. Upregulation of protein kinase B (Akt) is a critical factor in the progression of CRC [13]. It induces apoptosis *via* inhibition of rapidly accelerated fibrosarcoma (a family of three serine/threonine-specific protein kinases) – ERK activation [20].

In terms of benzimidazole, Nygre *et al.* [21] screened a compound library to identify agents with potential for repositioning in cancer therapy, and found that mebendazole and albendazole have anti-cancer activity in 80% of CRC cell lines. Benzimidazole inhibited the proliferation of HCT116 cells [22] and induced apoptosis *via* activated JNK in HCT116 and SW480 cells [23]. Flubendazole induced mitotic catastrophe with increased cyclin B1 and caspase-3-PARP pathway [24]. It has an anti-migratory effect by inhibiting the expression of nuclear factor kappa-light-chain-enhancer of activated B cells p65 in CRC cells derived from primary tumor and lymph node metastasis [25]. In addition, Williamson *et al.* [26] showed that mebendazole combined with non-steroidal anti-inflammatory drugs reduced tumor initiation by decreasing c-Myc and increasing apoptosis in an *Apc^{Min/+}* mouse model of familial adenomatous polyposis.

Although fenbendazole enhance the cytotoxicity of radiation or docetaxel and increased the anti-cancer effects of radiation against mammary tumors [27], only a few studies evaluated at the anti-cancer effects of benzimidazole against metastatic or resistant cancers [28-30]. Albendazole effectively inhibited paclitaxel- and doxorubicin-resistant lung cancer cells [31] and thereby reduced multidrug resistance. Nonetheless, the role of benzimidazole in resistant CRC has yet to be reported. Therefore, we aimed to evaluate the effects and underlying mechanisms of fenbendazole in SNU-C5/5-FUR cells as compared with wild type SNU-C5 cells in order to identify therapeutic strategies to overcome resistance to 5-FU.

METHODS

Reagents and antibodies

MTT was purchased from Amresco, Inc. (VWR International LLC, Seongnam, Korea). 5-fluorouracil (5-FU, #F6627), albendazole (#PHR 1281), deferoxamine mesylate (DFOM, #D9533), fenbendazole (#PHR 1832), and ferrostatin-1 (#SML 0583) were obtained from Sigma-Aldrich (Merck KGaA, Darmstadt, Germany).

Antibodies specific for c-Myc (9E10; #sc-40; diluted 1:1,000), cytochrome-C (H-104; #sc-7159; diluted 1:1,000), ERK (C-16; #sc-93; diluted 1:2,000), ferritin heavy chain (B-12) (FTH1; #sc-376594; diluted 1:2,000), GAPDH (#sc-47724; diluted 1:2,000),

and phospho-p53 (Ser6; #sc135630; diluted 1:1,000), transferrin receptor (H68.4) (TfRC; #sc-65882; diluted 1:2,000) were purchased from Santa Cruz Biotechnology (Santa Cruz, CA, USA); glutathione peroxidase 4 (GPX4 [EPNCIR144]; #ab125066; diluted 1:1,000) and SLC40A1 (ferroportin, FPN; #ab78066; diluted 1:1,000) were purchased from Abcam (Cambridge, UK); caspase-3 (#9665; diluted 1:1,000), cleaved caspase-3 (#9661; diluted 1:1,000), cyclin B1 (#4138; diluted 1:1,000), phospho-ERK (Thr202/Tyr204; #4370; diluted 1:2,000), JNK (#9252; diluted 1:1,000), phosphor-JNK (Thr183/Tyr185) (#9251; diluted 1:1,000), p21 (#2947; diluted 1:1,000), p27 (#2552; diluted 1:1,000), p38 MAPK (#9212; diluted 1:1,000), phospho-p38 MAPK (Thr180/Tyr182; #9211; diluted 1:1,000), PARP (#9542; diluted 1:1,000), autophagy antibody sampler kit (#4445; consisting of Beclin-1 (D40C5), LC3 (D3U4C), Atg5 (D5F5U), Atg12 (D88H11), Atg16L1 (D6D5), Atg7 (D12B11), and Atg3; diluted 1:2,000/each), and necroptosis antibody sampler kit (#98110; consisting of receptor-interacting protein kinase (RIP) (D94C12), phospho-RIP (Ser166) (D1L3S), mixed lineage kinase domain-like protein (MLKL) (D2I6N), phospho-MLKL (Ser358) (D6H3V), receptor-interacting protein kinase 3 (RIP3) (E1Z1d), and phospho-RIP3 (S227) (D6W2T); diluted 1:1,000/each) were purchased from Cell Signaling Technology Inc. (Beverly, MA, USA); the high mobility group box 1 (HMGB1; #GTX62170; diluted 1:2,000) and p53 (#GTX70218; diluted 1:1,000) were purchased from GeneTex (Irvine, CA, USA); SLC7A11 (cysteine/glutamate transporter; #ANT-111; diluted 1:2,000) was purchased from Alomone Labs (Jerusalem, Israel).

Cell culture and viability assay

SNU-C5 (IC_{50} against 5-FU = 5 μM) and the 5-fluorouracil-resistant SNU-C5 (SNU-C5/5-FUR; IC_{50} against 5-FU = 140 μM) cell lines were cultured as previously described [19,32].

To achieve similar confluency after 3 days of incubation, SNU-C5 (2×10^3 cells/well) and SNU-C5/5-FUR (5×10^3 cells/well) cells were seeded in 96-well plates. Cells were treated with benzimidazole (fenbendazole and albendazole) and anti-ferroptotic agents (ferrostatin-1 and DFOM) at various concentrations. The effect of drugs on cell viability was evaluated *via* reduction of MTT to its formazan product with a VERSAmax microplate reader (Molecular Devices Korea LLC, Seoul, Korea) as previously reported [19].

Flow cytometry

Cells were treated with or without fenbendazole (0.5 and 5.0 μM for SNU-C5 and SNU-C5/5-FUR cells, respectively) for 3 days, followed by flow cytometry using the FACSCalibur system (BD Biosciences, San Jose, CA, USA) and BD FACStation software version 6.0 (BD Biosciences) as described previously [19,32].

Western blotting analysis

The harvest, the protein quantification, and electrophoresis of the protein in cell lysates were performed as previously described [19,32]. The protein bands were captured and quantified using AzureSpot analysis software (version 14.2; Azure c300; Azure Biosystems, Inc., Dublin, CA, USA).

Statistical analysis

All data were compiled from a minimum of three replicate experiments. The data are expressed as mean values ± SD. Statistically significant differences (p < 0.05) were found using Student's paired t-test or one-way analysis of variance (ANOVA) with a Bonferroni *post-hoc* test (SPSS version 14.0; SPSS Inc., Chicago, IL, USA).
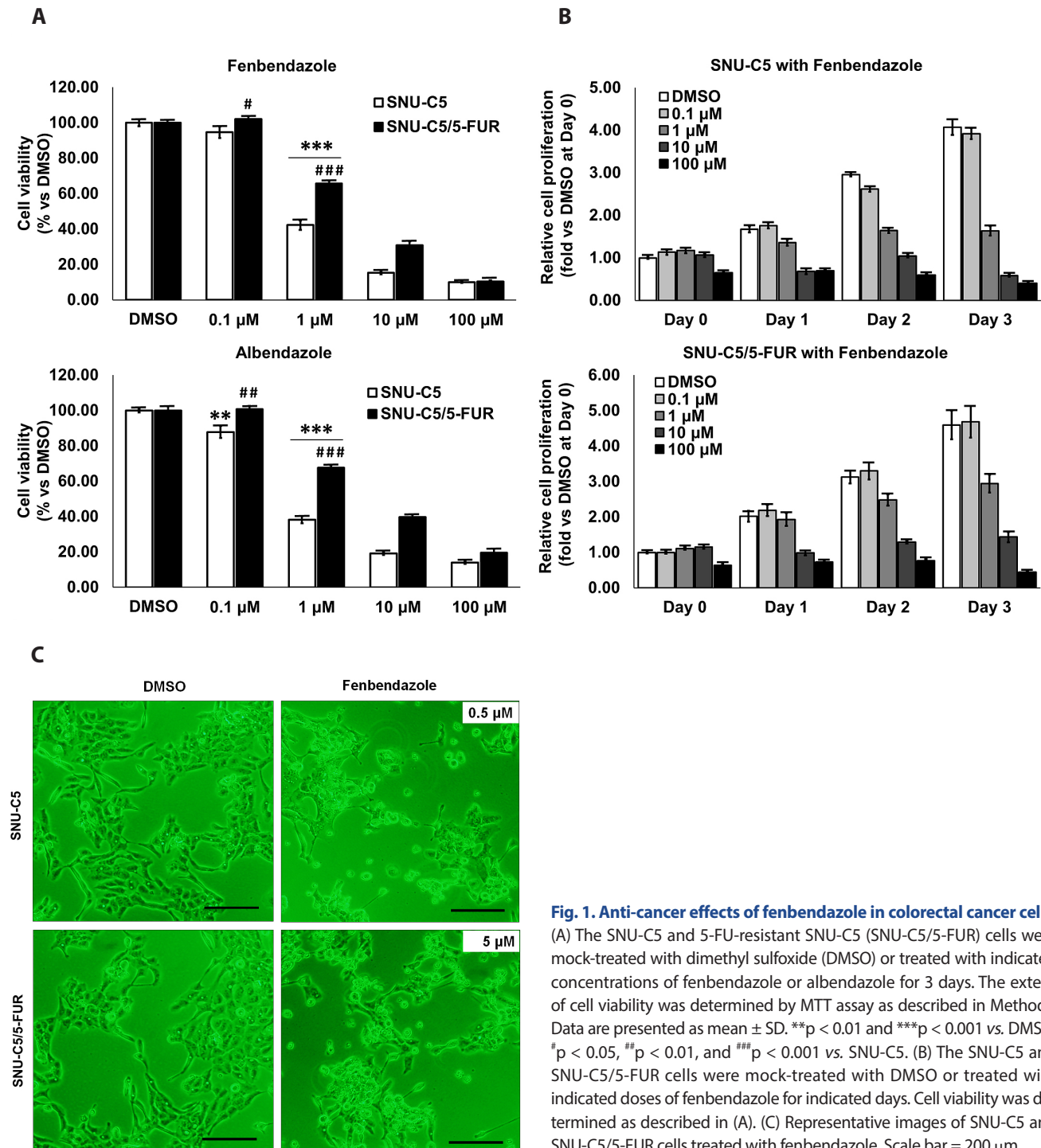

Fig. 1. Anti-cancer effects of fenbendazole in colorectal cancer cells. (A) The SNU-C5 and 5-FU-resistant SNU-C5 (SNU-C5/5-FUR) cells were mock-treated with dimethyl sulfoxide (DMSO) or treated with indicated concentrations of fenbendazole or albendazole for 3 days. The extent of cell viability was determined by MTT assay as described in Methods. Data are presented as mean ± SD. **p < 0.01 and ***p < 0.001 *vs.* DMSO. #p < 0.05, ##p < 0.01, and ###p < 0.001 *vs.* SNU-C5. (B) The SNU-C5 and SNU-C5/5-FUR cells were mock-treated with DMSO or treated with indicated doses of fenbendazole for indicated days. Cell viability was determined as described in (A). (C) Representative images of SNU-C5 and SNU-C5/5-FUR cells treated with fenbendazole. Scale bar = 200 μm.

RESULTS

Benzimidazole induced dose- and time-dependent anti-proliferative effects

Fenbendazole and albendazole showed dose-dependent anti-proliferative effects against both SNU-C5 and SNU-C5/5-FUR cells (Fig. 1A, C). After 3 days of incubation, the IC_{50} values of the SNU-C5 cells treated with fenbendazole and albendazole were 0.50 and 0.47 μM, respectively. The IC_{50} values of SNU-C5/5-FUR cells treated with fenbendazole and albendazole were 4.09 and 4.23 μM, respectively. Cell viability of SNU-C5 cells was s 42.24 ± 2.71% and 38.18 ± 2.01% when incubated with 1 μM of fenbendazole and albendazole, respectively. Cell viability of SNU-C5/5-FUR cells was 65.66 ± 1.83% and 67.57 ± 1.58% when treated with 1 μM of fenbendazole and albendazole, respectively, which was further decreased to 30.79 ± 2.35% and 39.78 ± 1.40% at 10 μM

concentrations.

Fenbendazole was more effective than albendazole against SNU-C5/5-FUR cells, and time-dependent anti-cancer effects of fenbendazole were further evaluated (Fig. 1B, C). Fenbendazole showed time-dependent anti-proliferative effects on both CRC cells. During 3 days of incubation, the proliferation of SNU-C5 cells increased 4.07 ± 0.18-fold with vehicle and 1.63 ± 0.11-fold with 1 μM of fenbendazole when compared with vehicle-treated control. During 3 days of incubation, SNU-C5/5-FUR cells proliferated 4.60 ± 0.41-fold with vehicle, and 2.94 ± 0.25 and 1.44 ± 0.15-fold with 1 μM and 10 μM of fenbendazole, respectively, when compared with vehicle-treated control. Taken together, a dose of close to the IC_{50} values of fenbendazole, 0.5 μM for SNU-C5 cells and 5 μM for SNU-C5/5-FUR cells, was used in subsequent experiments.
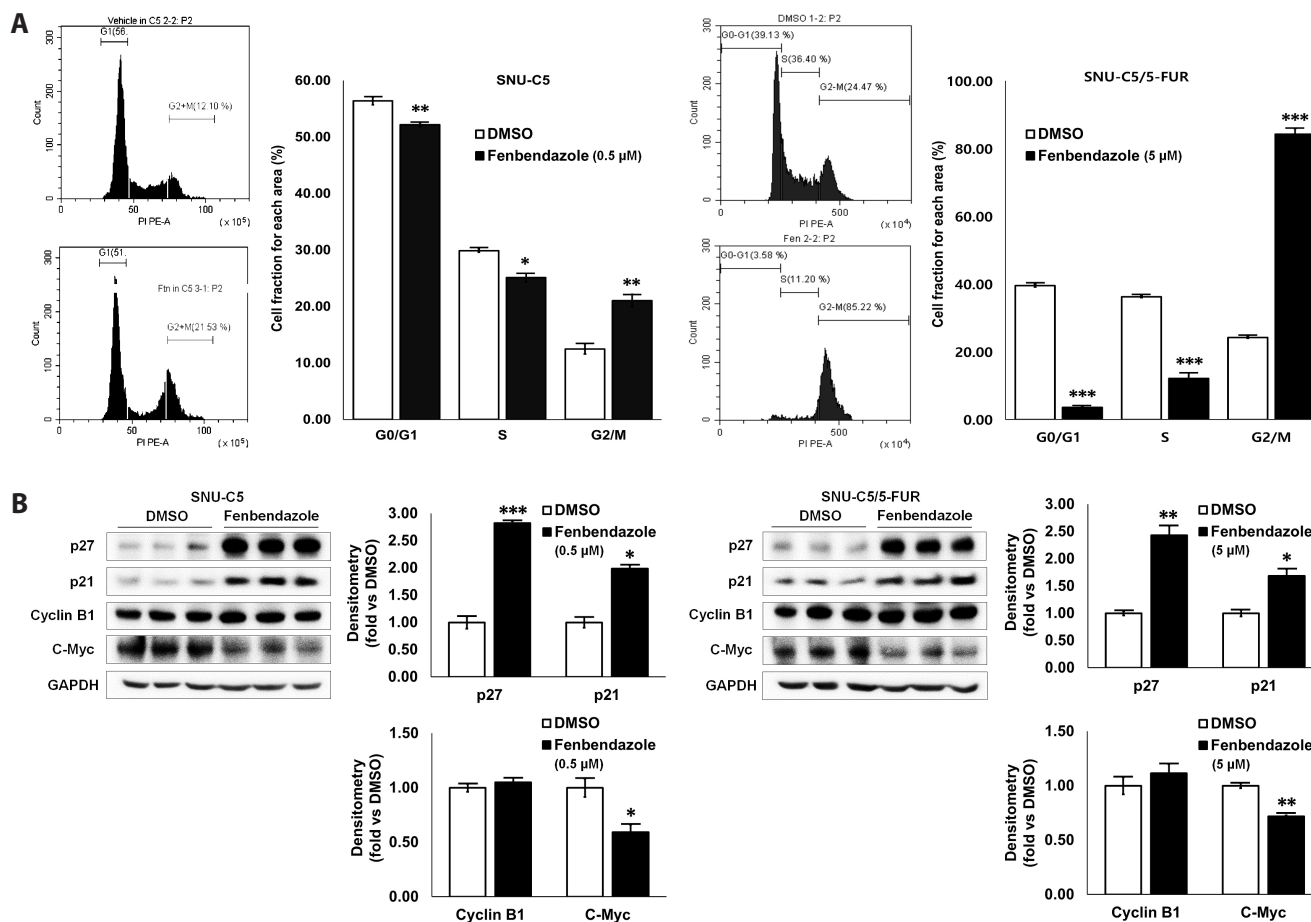

Fig. 2. Fenbendazole-induced cell cycle arrest at G2/M phase with increased p21 expression in colorectal cancer cells. (A) Cell cycle distribution in SNU-C5 and SNU-C5/5-FUR cells were assessed by flow cytometry after treatment with mock (dimethyl sulfoxide, DMSO) or indicated dose of fenbendazole for 3 days. The percentages of cells in each phase for SNU-C5 (*left*) and SNU-C5/5-FUR (*right*) cells are presented as the mean ± SD. *p < 0.05, **p < 0.01, and ***p < 0.001 *vs.* DMSO. (B) SNU-C5 (*left*) and SNU-C5/5-FUR (*right*) cells were mock-treated with DMSO or treated with indicated dose of fenbendazole. 3 days after treatment, cells were harvested and whole cell extracts were subjected to immunoblotting using the indicated antibodies. Signal intensities of p27, p21, Cyclin B1, and C-Myc were measured by AzureSpot analysis software. Data are presented as the mean ± SD. *p < 0.05, **p < 0.01, and ***p < 0.001 *vs.* DMSO.

Fenbendazole induced cell cycle arrest at G2/M phase with increased p21 expression on CRC cells

Cell cycle analysis resulted in a significant increase in the fraction of G2/M phase (Fig. 2A). The fraction of SNU-C5 (12.50 ± 0.92% *vs.* 21.07 ± 1.10%) and SNU-C5/5-FUR (24.24 ± 0.28% *vs.* 84.30 ± 1.66%) cells in the G2/M phase showed a significant upward trend, while the fraction of SNU-C5 (56.40 ± 0.69% *vs.* 52.20 ± 0.38%) and SNU-C5/5-FUR (39.53 ± 0.39% *vs.* 3.55 ± 0.13%) cells in the G0/G1 phase showed a significant downward trend. The proportion of S phase considerably decreased in SNU-C5 (29.91 ± 0.30% *vs.* 25.12 ± 0.77%) and SNU-C5/5-FUR (36.23 ± 0.24% *vs.* 12.15 ± 1.61%) cells.

Western blot revealed that p27 showed a significant increase in the number of SNU-C5 (2.82 ± 0.04-fold) and SNU-C5/5-FUR (2.43 ± 0.17-fold) cells. P21 expression was significantly increased in SNU-C5 (1.98 ± 0.07-fold) and SNU-C5/5-FUR (1.68 ± 0.13-fold) cells. Levels of c-Myc decreased considerably in SNU-C5

(0.59 ± 0.07-fold) and SNU-C5/5-FUR (0.72 ± 0.01-fold) cells, while cyclin B1 levels did not change considerably (Fig. 2B).

Fenbendazole induced apoptosis *via* caspase-3-PARP pathway in CRC cells

The cell death effects were identified *via* annexin V/PI staining after incubation with fenbendazole in SNU-C5 and SNU-C5/5-FUR cells (Fig. 3A). Cell death analysis showed a significant increase in the fraction of apoptosis and necrosis was found in both CRC cells compared with vehicle-treated cells (Fig. 3A). The fraction of SNU-C5 cells in early (1.24 ± 0.15% *vs.* 14.34 ± 0.26%) and late (3.95 ± 0.14% *vs.* 14.30 ± 0.08%) apoptosis along with the fraction of SNU-C5/5-FUR cells in early (0.25 ± 0.03% *vs.* 3.27 ± 0.14%) and late (1.83 ± 0.07% *vs.* 10.77 ± 0.72%) apoptosis showed a significant upward trend. The fraction of SNU-C5 (2.05 ± 0.09% *vs.* 7.59 ± 0.36%) and SNU-C5/5-FUR (1.40 ± 0.08% *vs.* 3.16 ± 0.16%) cells in necrosis also showed a significant upward trend.
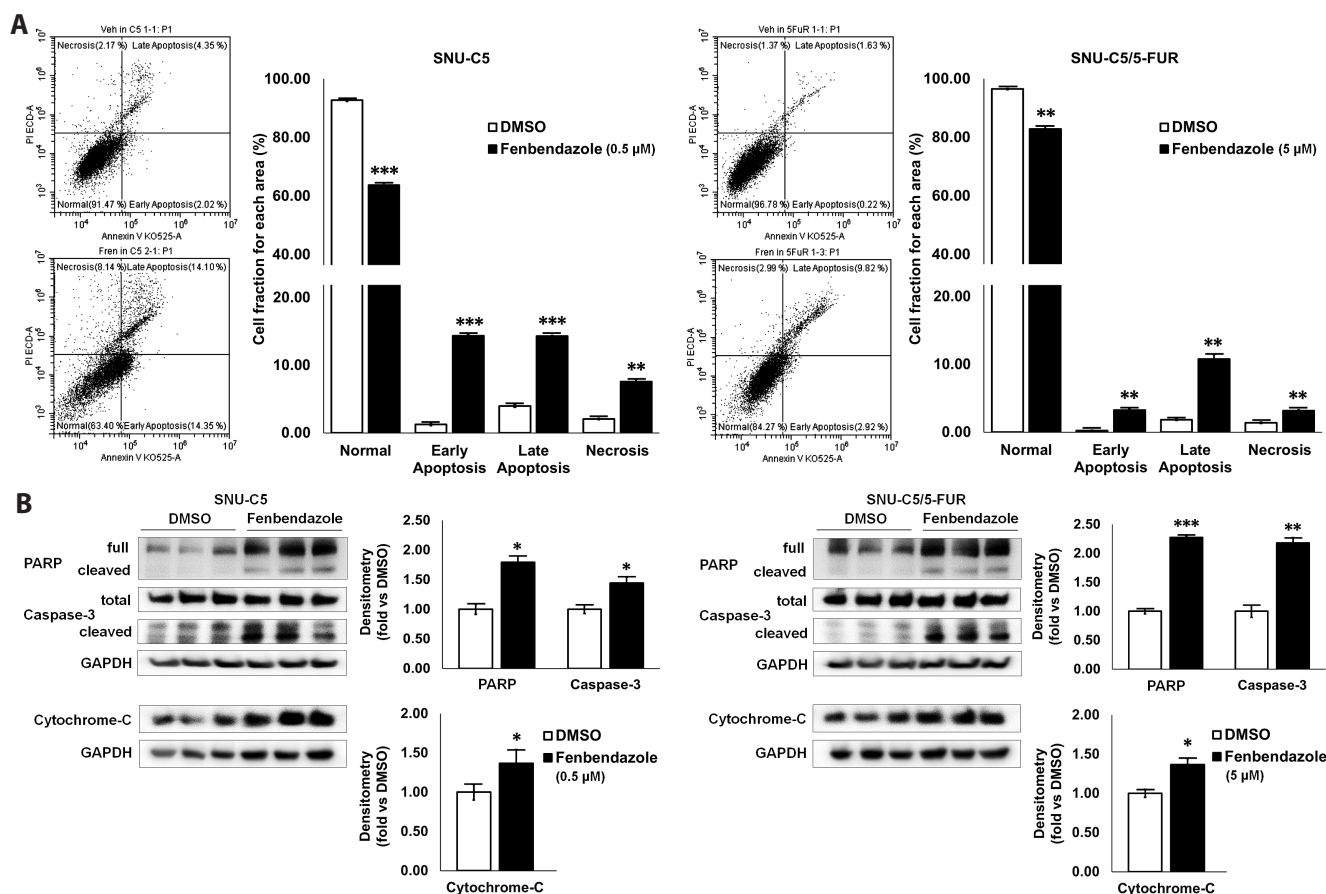

Fig. 3. Fenbendazole-induced apoptosis *via* mitochondrial injury and caspase-3-poly (ADP-ribose) polymerase (PARP) pathways in colorectal cancer cells. (A) Cell death distribution was assessed by annexin V/PI staining and flow cytometry after treatment with mock (dimethyl sulfoxide, DMSO) or indicated dose of fenbendazole for 3 days. The percentages of normal, early apoptosis, late apoptosis, and necrosis in SNU-C5 (*left*) and SNU-C5/5-FUR (*right*) cells are presented as the mean ± SD. **p < 0.01 and ***p < 0.001 *vs.* DMSO. (B) SNU-C5 and SNU-C5/5-FUR cells were mock-treated with DMSO or treated with indicated dose of fenbendazole. 3 days after treatment, cells were harvested and whole cell extracts were subjected to immunoblotting using the anti-PARP, anti-caspase-3, and anti-cytochrome C antibodies. Signal intensity of each proteins was measured by AzureSpot analysis software. Data are presented as the mean ± SD. *p < 0.05, **p < 0.01, and ***p < 0.001 *vs.* DMSO.

Western blot revealed that the activation (cleaved/full length) of PARP was significantly increased in SNU-C5 (1.79 ± 0.11-fold) and SNU-C5/5-FUR (2.28 ± 0.03-fold) cells. The activation (cleaved/total form) of caspase-3 was significantly increased in SNU-C5 (1.44 ± 0.10-fold) and SNU-C5/5-FUR (2.18 ± 0.09-fold) cells. The level of cytochrome-C showed a significant increase in SNU-C5 (1.37 ± 0.17-fold) and SNU-C5/5-FUR (1.37 ± 0.08-fold) cells (Fig. 3B).

Fenbendazole did not activate other cell death pathways in CRC cells

Western blot on autophagy proteins revealed that Beclin-1 expression was significantly increased in SNU-C5 (1.35 ± 0.02-fold) and SNU-C5/5-FUR (1.46 ± 0.07-fold) cells. LC3-I level increased slightly in SNU-C5 (1.13 ± 0.13-fold) cells but remained unchanged in SNU-C5/5-FUR cells. Atg7 expression increased considerably in SNU-C5 (1.53 ± 0.07-fold) and in SNU-C5/5-FUR (1.12 ± 0.06-fold) cells. Atg16L1 levels increased slightly in SNU-C5/5-FUR (1.21 ± 0.04-fold) but remained unchanged in SNU-C5 cells. Other markers were not changed considerably in both CRC cells (Fig. 4).

Western blot on ferroptosis proteins revealed that GPX4 showed significantly decreased levels in SNU-C5 (0.60 ± 0.02-fold) and SNU-C5/5-FUR (0.71 ± 0.05-fold) cells. FTH1 levels increased significantly in SNU-C5 (5.44 ± 0.32-fold) and SNU-

C5/5-FUR (3.48 ± 0.54-fold) cells. FPN showed a significant increase in SNU-C5 (1.77 ± 0.07-fold) and SNU-C5/5-FUR (1.59 ± 0.10-fold) cells. The levels of SLC7A11 increased slightly in SNU-C5 (1.19 ± 0.05-fold) cells but decreased significantly in SNU-C5/5-FUR (0.67 ± 0.02-fold) cells. The expression of transferrin receptor remained unchanged in both CRC cells. HMGB1, a member of damage-associated molecular patterns (DAMP), showed significantly increased levels in SNU-C5 (1.30 ± 0.10-fold) and SNU-C5/5-FUR (2.36 ± 0.06-fold) cells (Fig. 5A).

The effects of anti-ferroptotic agents, ferrostatin-1 and DFOM, were evaluated in fenbendazole-induced ferroptosis (Fig. 5B). Ferrostatin-1 co-treatment did not increase the viability of both CRC cells. Concentrations greater than 1 μM paradoxically decreased the cell viability in SNU-C5 (69.60 ± 4.85% vs. 47.10 ± 1.71%) and SNU-C5/5-FUR (75.95 ± 2.20% vs. 49.97 ± 1.15%) cells following co-treatment. Co-treatment with DFOM did not increase the viability of the CRC cells. High concentration (10 μM) of DFOM paradoxically decreased the viability of SNU-C5 (60.14 ± 2.11% vs. 35.33 ± 1.10%) and SNU-C5/5-FUR (73.04 ± 1.96% vs. 60.58 ± 1.61%) cells.

Western blot on necroptotic proteins revealed that the activation (phosphor/total) of RIP was significantly increased in SNU-C5 (2.31 ± 0.21-fold) and SNU-C5/5-FUR (4.72 ± 0.32-fold) cells. The activation of RIP3 was significantly decreased in SNU-C5 (0.42 ± 0.00-fold) and SNU-C5/5-FUR (0.47 ± 0.04-fold) cells. The activation of MLKL was not changed considerably in both
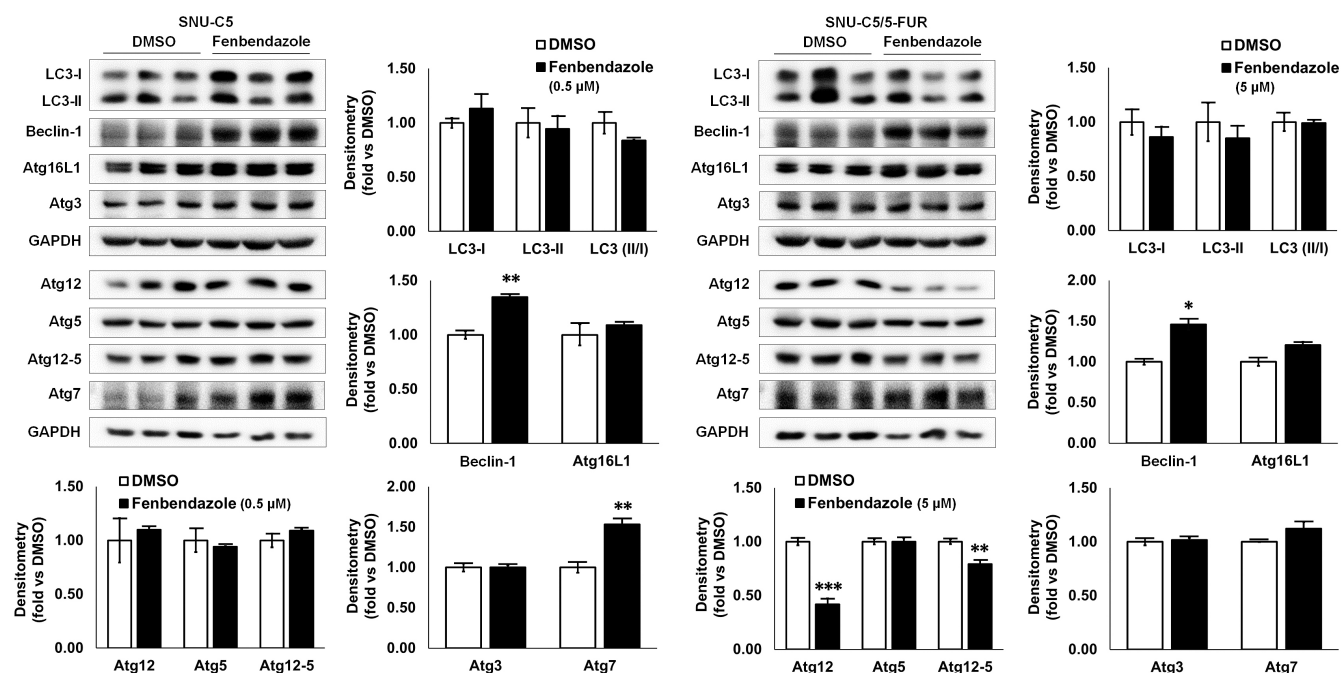

Fig. 4. Fenbendazole-induced autophagy *via* beclin-1 in colorectal cancer cells. Effect of fenbendazole on the expression of autophagy-related proteins in SNU-C5 and SNU-C5/5-FUR cells was detected by immunoblotting. SNU-C5 and SNU-C5/5-FUR cells were mock-treated with dimethyl sulfoxide (DMSO) or treated with indicated dose of fenbendazole for 3 days. Total protein was collected, and immunoblotting analysis was performed for light chain 3 (LC3) (I/II), Beclin-1, Atg16L1, Atg3, Atg5, Atg12 (detected Atg12-5 complex also), and Atg7. GAPDH was used for a loading control. Band density was analyzed by AzureSpot analysis software, and results are expressed as the mean ± SD. *p < 0.05, **p < 0.01 *vs.* DMSO.
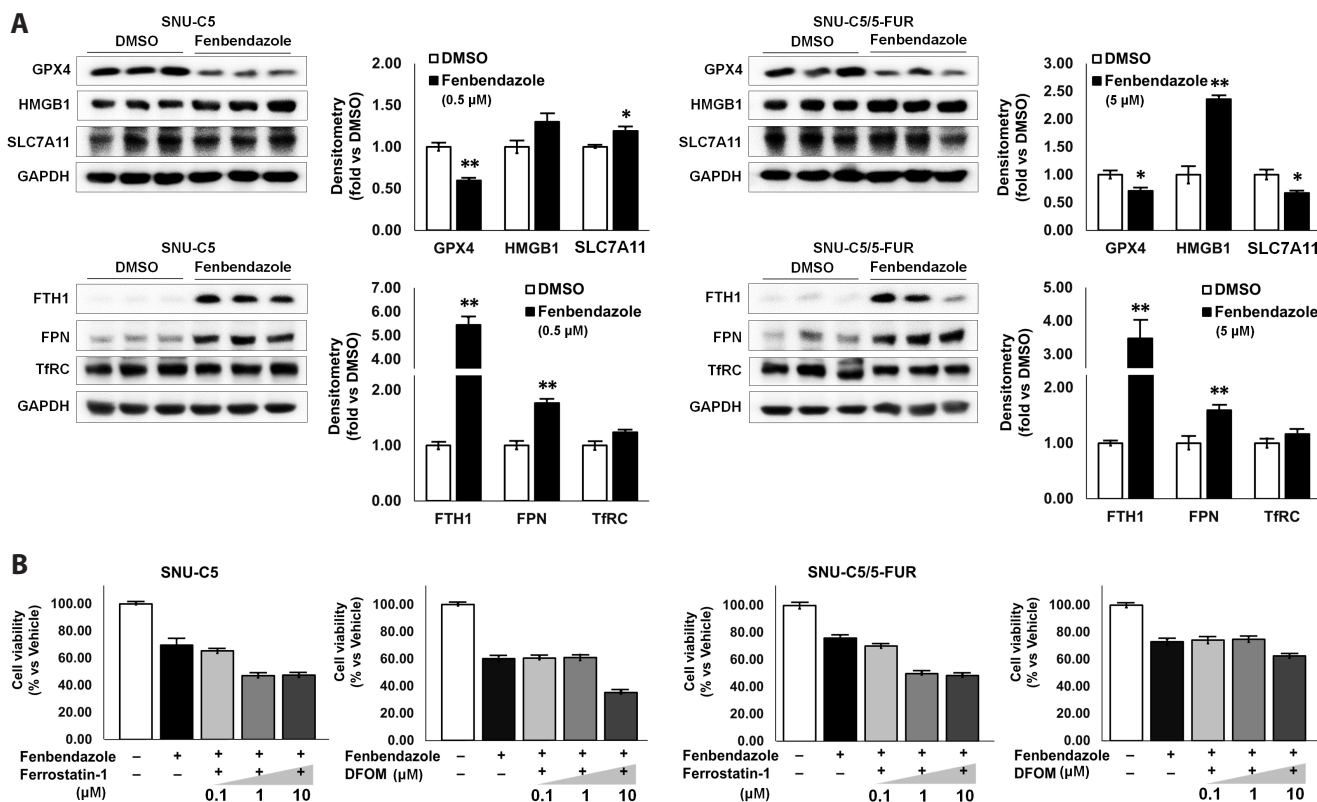
Fig. 5. Fenbendazole-induced ferroptosis *via* glutathione peroxidase 4 (GPX4) in colorectal cancer cells. (A) Effect of fenbendazole on the expression of ferroptosis-related proteins in SNU-C5 and SNU-C5/5-FUR cells was detected by immunoblotting. SNU-C5 and SNU-C5/5-FUR cells were mock-treated with dimethyl sulfoxide (DMSO) or treated with indicated dose of fenbendazole for 3 days. Total protein was collected, and immunoblotting analysis was performed for GPX4, high mobility group box 1 (HMGB1), SCL7A11, ferritin heavy chain (FTH1), ferroportin (FPN), and transferrin receptor (TfRC). GAPDH was used for a loading control. Band density was analyzed by AzureSpot analysis software, and results are expressed as the mean ± SD. *$p < 0.05$, **$p < 0.01$ *vs.* DMSO. (B) The SNU-C5 and SNU-C5/5-FUR cells were treated with fenbendazole alone or with fenbendazole in combination with indicated doses of ferrostatin-1 or deferoxamine mesylate (DFOM) for 3 days. The extent of cell viability was determined by MTT assay. Data are presented as mean ± SD.

CRC cells (Fig. 6). While the full length of caspase-8 was not changed in both CRC cells, the significant increase was observed in the active cleaved fragment in SNU-C5 (2.45 ± 0.21-fold) cells and the cleaved intermediate fragment in SNU-C5/5-FUR (1.22 ± 0.07-fold) cells (Fig. 6).

Fenbendazole activated p53 on SNU-C5 cells, but not on SNU-C5/5-FUR cells

The activation (phosphor/total form) of p53 was significantly increased in SNU-C5 (1.17 ± 0.05-fold) cells, but the activation of p38, ERK, and JNK did not change. The activation of p53, p38 (0.83 ± 0.02-fold), ERK, and JNK showed no significant changes in SNU-C5/5-FUR cells (Fig. 7).

DISCUSSION

As reported previously [1,30], we found that fenbendazole arrests cell cycle at G2/M phase and induces apoptosis *via* p53-p21

pathways in SNU-C5 and SNU-C5/5-FUR cells. Cell death pathways were further investigated in terms of apoptosis, autophagy, ferroptosis, and necroptosis to identify the differences in 5-FU resistance. Benzimidazoles induce apoptosis *via* caspase-3-PARP activation [1], which is also true in SNU-C5 and SNU-C5/5-FUR cells with the increased levels of mitochondrial injury marker, cytochrome-C. Benzimidazole is historically known to bind beta-tubulin, disrupt microtubules, and arrest cell division [1,30,33-35]. Although Beclin-1 was increased in SNU-C5 and SNU-C5/5-FUR cells, autophagy might be not so effective due to insufficient LC3 (II/I) activation especially in SNU-C5/5-FUR cells.

Benzimidazole-induced ferroptosis has yet to be fully reported. Ferroptosis is characterized by lipid peroxidation. It can be induced by the accumulation of free iron and *via* the inactivation of cysteine uptake by SLC7A11 or the inactivation of the lipid repair enzyme GPX4 [36-38]. Free iron level might be regulated (decreased) by the increased expression of FTH1 (storage) and FPN (exporter), whereas decreased expression of GPX4 and/or SLC7A11 induces ferroptosis in SNU-C5 and SNU-C5/5-FUR cells. The effects of anti-ferroptotic agents were elucidated to establish
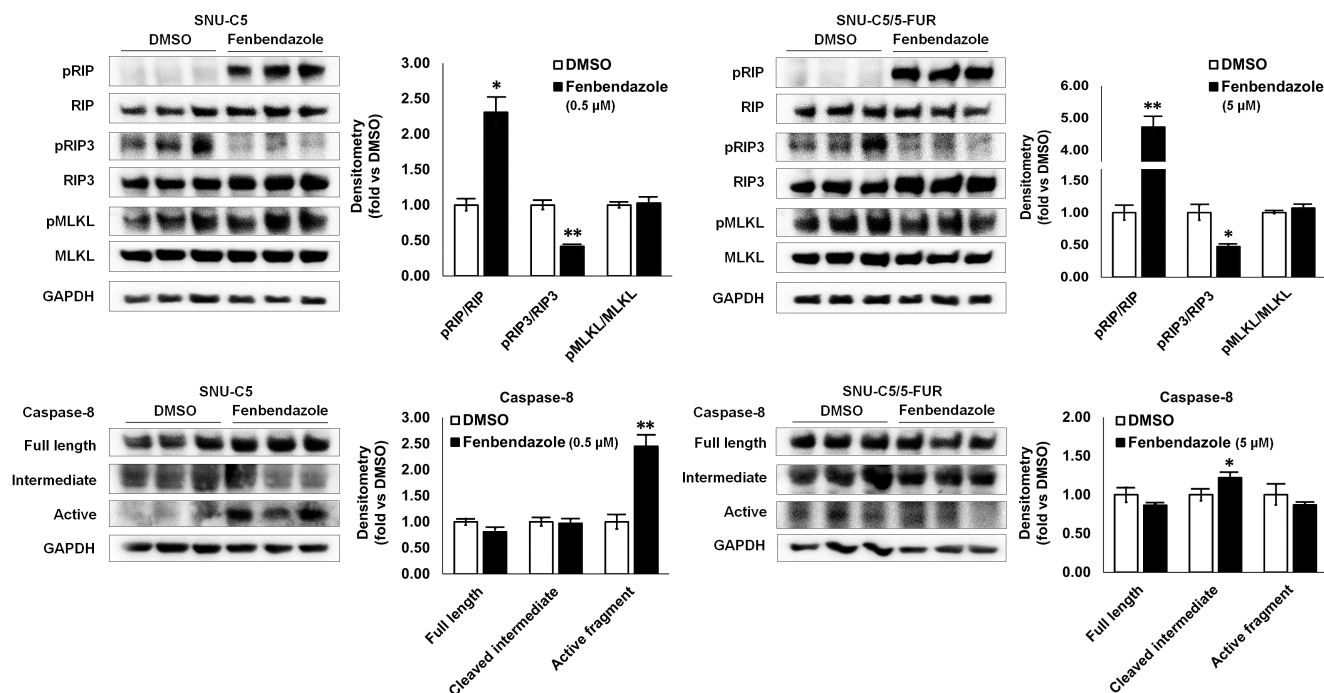
Fig. 6. Fenbendazole-induced necroptosis in colorectal cancer cells. Effect of fenbendazole on the expression of necroptosis-related proteins in SNU-C5 and SNU-C5/5-FUR cells was detected by immunoblotting. SNU-C5 and SNU-C5/5-FUR cells were mock-treated with dimethyl sulfoxide (DMSO) or treated with indicated dose of fenbendazole for 3 days. Total protein was collected, and immunoblotting analysis was performed for phospho-receptor-interacting protein kinase (pRIP), RIP, pRIP3, RIP3, phosphor-mixed lineage kinase domain-like protein (pMLKL), MLKL, and caspase-8. GAPDH was used for a loading control. Band density was analyzed by AzureSpot analysis software, and results are expressed as the mean ± SD. *p < 0.05, **p < 0.01 *vs.* DMSO.
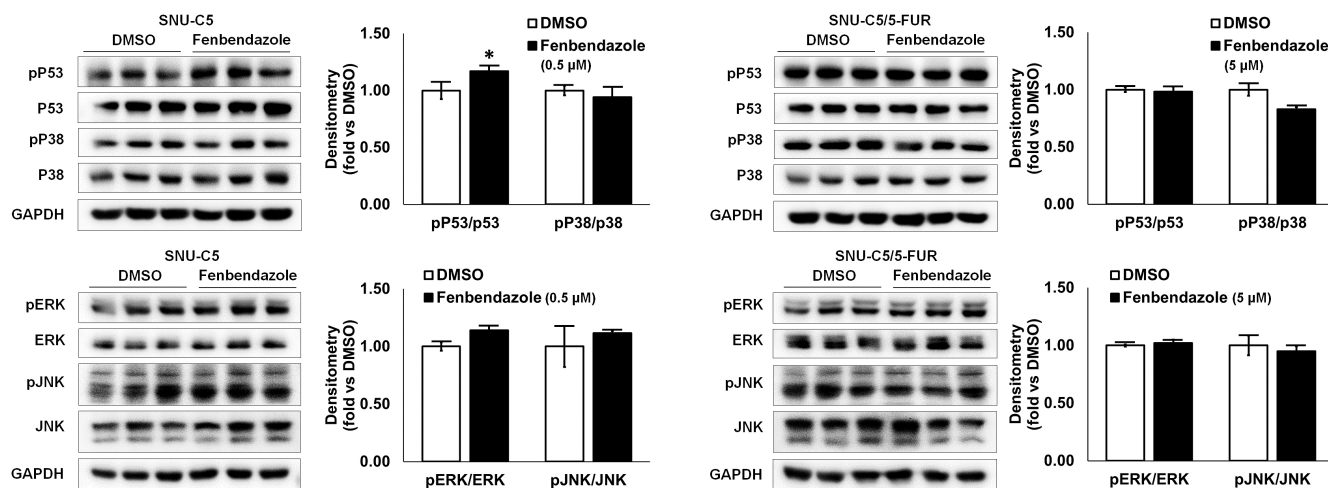

Fig. 7. Fenbendazole-induced p53 activation in colorectal cancer cells. SNU-C5 and SNU-C5/5-FUR cells were mock-treated with dimethyl sulfoxide (DMSO) or treated with indicated dose of fenbendazole. 3 days after treatment, cells were harvested and whole cell extracts were subjected to immunoblotting using the indicated antibodies. Signal intensity of each proteins was measured by AzureSpot analysis software. Data are presented as the mean ± SD. *p < 0.05 *vs.* DMSO.

ferroptosis as main cell death pathway in fenbendazole treatment. Treatment with ferrostatin-1 (the inhibitor of SLC7A11-dependent ferroptosis) and DFOM (the iron chelating agent to inhibit ferroptosis) did not effectively block the fenbendazole-induced cell viability, suggesting that ferroptosis is not the primary cell death

pathway in fenbendazole-induced anti-cancer effects. However, ferroptosis-inducing agents trigger synergistic apoptosis by increasing DAMP as reported in HCT116 cells [39].

Benzimidazole-related necroptosis has yet to be investigated comprehensively. Necroptosis is negatively regulated by caspases

and initiated by a complex containing of RIP and RIP3 kinases, leading to phosphorylation of MLKL [40-42]. In this study, MLKL activation was not affected by fenbendazole treatment, and thus necroptosis was not effectively activated in both CRC cells. But active and intermediate form of caspase-8 was increased in SNU-C5 and SNU-C5/5-FUR cells, respectively, which induces apoptosis *via* cytochrome-C or caspase-3 [43].

During MAPK signaling, benzimidazole usually inhibits ERK activation [7,44], but increases p38 [5,35] and JNK activation [5,23,33,35,45]. Interestingly, ERK-dependent activation of heat shock factor-1 (HSF-1) promotes chemotherapeutic resistance to benzimidazole (parbendazole and nocodazole) in HCT116 and RKO cells. Biochemical inhibition of HSF-1 results in significant enhancement of drug potency. Therefore, Wales *et al.* [34] suggested that targeting ERK signaling pathway is a potential strategy in benzimidazole-resistant CRC cells. Despite the contrasting ERK response to yeast extract treatment in SNU-C5 and SNU-C5/5-FUR cells [19], we found no significant changes on p38, ERK and JNK, signaling after fenbendazole treatment.

Benzimidazole is known to activate p53 and p21 but decrease mutant p53 expression [30,46]. Cancer cells with wild-type p53 showed higher sensitivity to fenbendazole compared with p53 mutant cells [5,35]. In addition to cell cycle arrest *via* p53-p21 pathways [1,30,47], p53 acts as a key metabolic switch in cellular function and death [48-50]. In this study, fenbendazole induces G2/M arrest and apoptosis in both 5-FU-sensitive SNU-C5 and SNU-C5/5-FUR CRC cells. In SNU-C5 cells, fenbendazole is presumed to activate p53-mediated apoptosis by increasing p53 expression, and partly necrosis, autophagy and ferroptosis (Fig. 8A). P53 activation is mainly associated with mitochondrial injury and caspase-3-dependent apoptosis, of which caspase-3 activation might be partly induced by caspase-8 and Beclin-1. In addition,

ferroptosis by decreased GPX4 might augment apoptosis as previously described [39]. In SNU-C5/5-FUR cells, fenbendazole triggers apoptosis without affecting p53 expression (Fig. 8B), which was characterized by the following differences as compared with SNU-C5 cells. The expression of LC3, Atg7, and active caspase-8 was not increased, which resulted in reduced autophagy and caspase-8-dependent apoptosis. The expression of SLC7A11 as well as GPX4 was suppressed, which resulted in ferroptosis as previously reported [51,52]. As a result, apoptosis was partly induced by Beclin-1, and further augmented by ferroptosis in SNU-C5/5-FUR cells than in SNU-C5 cells. However, the activation of p53 with benzimidazole treatment is still disputed. Benzimidazole induces concurrent apoptosis and pyroptosis of human glioblastoma cells as well as inhibits cell cycle *via* p53-p21 pathway [53], while mebendazole was associated with p53-independent induction of p21 and tubule depolymerization in ovarian cancer [54]. Therefore, cell-type specific activation of p53 should be identified prior to benzimidazole, including fenbendazole, treatment of various cancers.

Taken together, SNU-C5/5-FUR cells exhibited approximately 10-fold higher IC_{50} values with fenbendazole compared with SNU-C5 cells, but still showed cytotoxicity at micromolar concentrations as previously reported [35]. Fenbendazole induces apoptosis as well as cell cycle arrest at G2/M phase *via* p53-p21 pathways in CRC cells. In case of cell death, fenbendazole induces primarily apoptotic cell death rather than autophagy, ferroptosis, and necroptosis. Although fenbendazole has anti-cancer effects on both 5-FU-sensitive and resistant CRC cells, the mechanism of action appears to be different. That is, fenbendazole promotes cell death by activating p53-mediated apoptosis in SNU-C5 cells, whereas by both enhancing p53-independent apoptosis and ferroptosis-augmented apoptosis in SNU-C5/5-FUR cells. There-
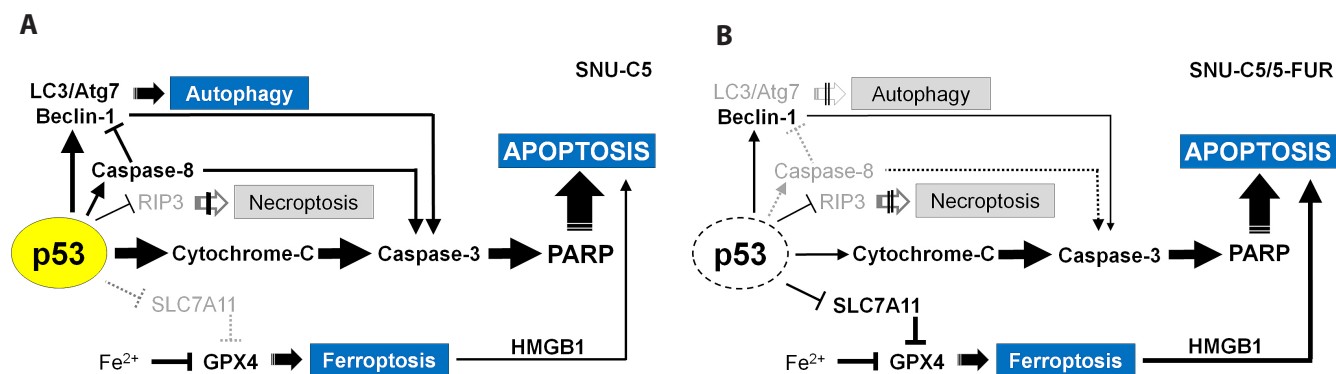

Fig. 8. Schematic representation of cell death pathways in colorectal cancer (CRC) cells following fenbendazole treatment. Fenbendazole induces G2/M arrest and apoptosis in both (A) 5-FU-sensitive SNU-C5 and (B) 5-FU-resistant SNU-C5 (SNU-C5/5-FUR) CRC cells. In SNU-C5 cells, fenbendazole is presumed to activate p53-mediated apoptosis by increasing p53 expression. In SNU-C5/5-FUR cells, fenbendazole triggers apoptosis without affecting p53 expression, whereas fenbendazole enhances ferroptosis by inhibiting the expression of GPX4 and SLC7A11. Therefore, although fenbendazole has anti-cancer effects on both 5-FU-sensitive and resistant CRC cells, the mechanism of action appears to be different. That is, fenbendazole promotes cell death by activating p53-mediated apoptosis in SNU-C5 cells, whereas by both enhancing p53-independent apoptosis and ferroptosis-augmented apoptosis in SNU-C5/5-FUR cells. PARP, poly (ADP-ribose) polymerase; HMGB1, high mobility group box 1; GPX4, glutathione peroxidase 4; LC3, light chain 3.

fore, further studies are needed to identify sensitive and resistant cancer cell types to facilitate cell type-specific treatment with benzimidazole.

FUNDING

ACKNOWLEDGEMENTS

None.

CONFLICTS OF INTEREST

The authors declare no conflicts of interest.

REFERENCES

1. Son DS, Lee ES, Adunyah SE. The antitumor potentials of benzimidazole anthelmintics as repurposing drugs. *Immune Netw.* 2020;20:e29.
2. Mukhopadhyay T, Sasaki J, Ramesh R, Roth JA. Mebendazole elicits a potent antitumor effect on human cancer cell lines both *in vitro* and *in vivo*. *Clin Cancer Res.* 2002;8:2963-2969.
3. Sasaki J, Ramesh R, Chada S, Gomyo Y, Roth JA, Mukhopadhyay T. The anthelmintic drug mebendazole induces mitotic arrest and apoptosis by depolymerizing tubulin in non-small cell lung cancer cells. *Mol Cancer Ther.* 2002;1:1201-1209.
4. Martarelli D, Pompei P, Baldi C, Mazzoni G. Mebendazole inhibits growth of human adrenocortical carcinoma cell lines implanted in nude mice. *Cancer Chemother Pharmacol.* 2008;61:809-817.
5. Dogra N, Mukhopadhyay T. Impairment of the ubiquitin-proteasome pathway by methyl N-(6-phenylsulfanyl-1H-benzimidazol-2-yl)carbamate leads to a potent cytotoxic effect in tumor cells: a novel antiproliferative agent with a potential therapeutic implication. *J Biol Chem.* 2012;287:30625-30640.
6. Lin S, Yang L, Yao Y, Xu L, Xiang Y, Zhao H, Wang L, Zuo Z, Huang X, Zhao C. Flubendazole demonstrates valid antitumor effects by inhibiting STAT3 and activating autophagy. *J Exp Clin Cancer Res.* 2019;38:293.
7. Michaelis M, Agha B, Rothweiler F, Löschmann N, Voges Y, Mittelbronn M, Starzetz T, Harter PN, Abhari BA, Fulda S, Westermann F, Riecken K, Spek S, Langer K, Wiese M, Dirks WG, Zehner R, Cinatl J, Wass MN, Cinatl J Jr. Identification of flubendazole as potential anti-neuroblastoma compound in a large cell line screen. *Sci Rep.* 2015;5:8202.
8. Heo DS. Anthelmintics as potential anti-cancer drugs? *J Korean Med Sci.* 2020;35:e75.
9. Yamaguchi T, Shimizu J, Oya Y, Horio Y, Hida T. Drug-induced liver injury in a patient with nonsmall cell lung cancer after the self-administration of fenbendazole based on social media information. *Case Rep Oncol.* 2021;14:886-891.
10. Chiang RS, Syed AB, Wright JL, Montgomery B, Srinlavs S. Fenbendazole enhancing anti-tumor effect: a case series. Clin Oncol Case Rep. 2021;4:2.
11. Bray F, Ferlay J, Soerjomataram I, Siegel RL, Torre LA, Jemal A. Global cancer statistics 2018: GLOBOCAN estimates of incidence and mortality worldwide for 36 cancers in 185 countries. *CA Cancer J Clin.* 2018;68:394-424. Erratum in: *CA Cancer J Clin.* 2020;70:313.
12. Azwar S, Seow HF, Abdullah M, Faisal Jabar M, Mohtarrudin N. Recent updates on mechanisms of resistance to 5-fluorouracil and reversal strategies in colon cancer treatment. *Biology (Basel).* 2021; 10:854.
13. Pan MH, Lai CS, Wu JC, Ho CT. Molecular mechanisms for chemoprevention of colorectal cancer by natural dietary compounds. *Mol Nutr Food Res.* 2011;55:32-45.
14. Fridman JS, Lowe SW. Control of apoptosis by p53. *Oncogene.* 2003;22:9030-9040.
15. Li XL, Zhou J, Chen ZR, Chng WJ. P53 mutations in colorectal cancer- molecular pathogenesis and pharmacological reactivation. *World J Gastroenterol.* 2015;21:84-93.
16. Thornton TM, Rincon M. Non-classical p38 map kinase functions: cell cycle checkpoints and survival. *Int J Biol Sci.* 2009;5:44-51.
17. Grossi V, Peserico A, Tezil T, Simone C. p38α MAPK pathway: a key factor in colorectal cancer therapy and chemoresistance. *World J Gastroenterol.* 2014;20:9744-9758.
18. Kim EJ, Kang JI, Kwak JW, et al. The anticancer effect of (1S,2S,3E,7E,11E)-3,7,11, 15-cembratetraen-17,2-olide(LS-1) through the activation of TGF-β signaling in SNU-C5/5-FU, fluorouracil-resistant human colon cancer cells. *Mar Drugs.* 2015;13:1340-1359.
19. Moon D, Kang HK, Kim J, Yoon SP. Yeast extract induces apoptosis and cell cycle arrest via activating p38 signal pathway in colorectal cancer cells. *Ann Clin Lab Sci.* 2020;50:31-44.
20. Arkun Y. Dynamic modeling and analysis of the cross-talk between insulin/AKT and MAPK/ERK signaling pathways. *PLoS One.* 2016; 11:e0149684.
21. Nygren P, Fryknäs M, Agerup B, Larsson R. Repositioning of the anthelmintic drug mebendazole for the treatment for colon cancer. *J Cancer Res Clin Oncol.* 2013;139:2133-2140.
22. Al-Douh MH, Sahib HB, Osman H, Abd Hamid S, Salhimi SM. Anti-proliferation effects of benzimidazole derivatives on HCT-116 colon cancer and MCF-7 breast cancer cell lines. *Asian Pac J Cancer Prev.* 2012;13:4075-4079.
23. Chen K, Chu BZ, Liu F, Li B, Gao CM, Li LL, Sun QS, Shen ZF, Jiang YY. New benzimidazole acridine derivative induces human colon cancer cell apoptosis *in vitro via* the ROS-JNK signaling pathway. *Acta Pharmacol Sin.* 2015;36:1074-1084.
24. Králová V, Hanušová V, Rudolf E, Čáňová K, Skálová L. Flubendazole induces mitotic catastrophe and senescence in colon cancer cells in vitro. *J Pharm Pharmacol.* 2016;68:208-218.
25. Hanušová V, Skálová L, Králová V, Matoušková P. The effect of flubendazole on adhesion and migration in SW480 and SW620 colon cancer cells. *Anticancer Agents Med Chem.* 2018;18:837-846.
26. Williamson T, Bai RY, Staedtke V, Huso D, Riggins GJ. Mebendazole and a non-steroidal anti-inflammatory combine to reduce tumor initiation in a colon cancer preclinical model. *Oncotarget.*

2016;7:68571-68584.

27. Duan Q, Liu Y, Rockwell S. Fenbendazole as a potential anticancer drug. *Anticancer Res.* 2013;33:355-362.

28. Doudican N, Rodriguez A, Osman I, Orlow SJ. Mebendazole induces apoptosis via Bcl-2 inactivation in chemoresistant melanoma cells. *Mol Cancer Res.* 2008;6:1308-1315.

29. Bai RY, Staedtke V, Aprhys CM, Gallia GL, Riggins GJ. Antiparasitic mebendazole shows survival benefit in 2 preclinical models of glioblastoma multiforme. *Neuro Oncol.* 2011;13:974-982.

30. Mrkvová Z, Uldrijan S, Pombinho A, Bartůněk P, Slaninová I. Benzimidazoles downregulate Mdm2 and MdmX and activate p53 in MdmX overexpressing tumor cells. *Molecules.* 2019;24:2152.

31. Tang Y, Liang J, Wu A, Chen Y, Zhao P, Lin T, Zhang M, Xu Q, Wang J, Huang Y. Co-delivery of trichosanthin and albendazole by nano-self-assembly for overcoming tumor multidrug-resistance and metastasis. *ACS Appl Mater Interfaces.* 2017;9:26648-26664. Erratum in: *ACS Appl Mater Interfaces.* 2020;12:3275.

32. Kim JW, Kim SH, Mariappan R, Moon D, Kim J, Yoon SP. Anticancer effects of the aqueous extract of Orostachys japonica A. Berger on 5-fluorouracil-resistant colorectal cancer via MAPK signalling pathways in vitro and in vivo. *J Ethnopharmacol.* 2021;280:114412.

33. Feng R, Li S, Lu C, Andreas C, Stolz DB, Mapara MY, Lentzsch S. Targeting the microtubular network as a new antimyeloma strategy. *Mol Cancer Ther.* 2011;10:1886-1896.

34. Wales CT, Taylor FR, Higa AT, McAllister HA, Jacobs AT. ERK-dependent phosphorylation of HSF1 mediates chemotherapeutic resistance to benzimidazole carbamates in colorectal cancer cells. *Anticancer Drugs.* 2015;26:657-666.

35. Dogra N, Kumar A, Mukhopadhyay T. Fenbendazole acts as a moderate microtubule destabilizing agent and causes cancer cell death by modulating multiple cellular pathways. *Sci Rep.* 2018;8:11926.

36. Yang WS, SriRamaratnam R, Welsch ME, Shimada K, Skouta R, Viswanathan VS, Cheah JH, Clemons PA, Shamji AF, Clish CB, Brown LM, Girotti AW, Cornish VW, Schreiber SL, Stockwell BR. Regulation of ferroptotic cancer cell death by GPX4. *Cell.* 2014;156:317-331.

37. Friedmann Angeli JP, Schneider M, Proneth B, Tyurina YY, Tyurin VA, Hammond VJ, Herbach N, Aichler M, Walch A, Eggenhofer E, Basavarajappa D, Rådmark O, Kobayashi S, Seibt T, Beck H, Neff F, Esposito I, Wanke R, Förster H, Yefremova O, *et al.* Inactivation of the ferroptosis regulator Gpx4 triggers acute renal failure in mice. *Nat Cell Biol.* 2014;16:1180-1191.

38. Latunde-Dada GO. Ferroptosis: role of lipid peroxidation, iron and ferritinophagy. *Biochim Biophys Acta Gen Subj.* 2017;1861:1893-1900.

39. Lee YS, Lee DH, Jeong SY, Park SH, Oh SC, Park YS, Yu J, Choudry HA, Bartlett DL, Lee YJ. Ferroptosis-inducing agents enhance TRAIL-induced apoptosis through upregulation of death receptor 5. *J Cell Biochem.* 2019;120:928-939.

40. Kaczmarek A, Vandenabeele P, Krysko DV. Necroptosis: the release

of damage-associated molecular patterns and its physiological relevance. *Immunity.* 2013;38:209-223.

41. Cai Z, Jitkaew S, Zhao J, Chiang HC, Choksi S, Liu J, Ward Y, Wu LG, Liu ZG. Plasma membrane translocation of trimerized MLKL protein is required for TNF-induced necroptosis. *Nat Cell Biol.* 2014;16:55-65. Erratum in: *Nat Cell Biol.* 2014;16:200.

42. Nirmala JG, Lopus M. Cell death mechanisms in eukaryotes. *Cell Biol Toxicol.* 2020;36:145-164.

43. Zhong B, Liu M, Bai C, Ruan Y, Wang Y, Qiu L, Hong Y, Wang X, Li L, Li B. Caspase-8 induces lysosome-associated cell death in cancer cells. *Mol Ther.* 2020;28:1078-1091.

44. Younis NS, Ghanim AMH, Saber S. Mebendazole augments sensitivity to sorafenib by targeting MAPK and BCL-2 signalling in n-nitrosodiethylamine-induced murine hepatocellular carcinoma. *Sci Rep.* 2019;9:19095.

45. Zhang F, Li Y, Zhang H, Huang E, Gao L, Luo W, Wei Q, Fan J, Song D, Liao J, Zou Y, Liu F, Liu J, Huang J, Guo D, Ma C, Hu X, Li L, Qu X, Chen L, *et al.* Anthelmintic mebendazole enhances cisplatin's effect on suppressing cell proliferation and promotes differentiation of head and neck squamous cell carcinoma (HNSCC). *Oncotarget.* 2017;8:12968-12982.

46. Xu D, Tian W, Jiang C, Huang Z, Zheng S. The anthelmintic agent oxfendazole inhibits cell growth in non-small cell lung cancer by suppressing c-Src activation. *Mol Med Rep.* 2019;19:2921-2926.

47. Mirzayans R, Andrais B, Scott A, Murray D. New insights into p53 signaling and cancer cell response to DNA damage: implications for cancer therapy. *J Biomed Biotechnol.* 2012;2012:170325.

48. Wang DB, Kinoshita C, Kinoshita Y, Morrison RS. p53 and mitochondrial function in neurons. *Biochim Biophys Acta.* 2014;1842:1186-1197.

49. Moulder DE, Hatoum D, Tay E, Lin Y, McGowan EM. The roles of p53 in mitochondrial dynamics and cancer metabolism: the pendulum between survival and death in breast cancer? *Cancers (Basel).* 2018;10:189.

50. Tang D, Kang R, Berghe TV, Vandenabeele P, Kroemer G. The molecular machinery of regulated cell death. *Cell Res.* 2019;29:347-364.

51. Kang R, Kroemer G, Tang D. The tumor suppressor protein p53 and the ferroptosis network. *Free Radic Biol Med.* 2019;133:162-168.

52. Lei G, Mao C, Yan Y, Zhuang L, Gan B. Ferroptosis, radiotherapy, and combination therapeutic strategies. *Protein Cell.* 2021;12:836-857.

53. Ren LW, Li W, Zheng XJ, Liu JY, Yang YH, Li S, Zhang S, Fu WQ, Xiao B, Wang JH, Du GH. Benzimidazoles induce concurrent apoptosis and pyroptosis of human glioblastoma cells via arresting cell cycle. *Acta Pharmacol Sin.* 2022;43:194-208.

54. Elayapillai S, Ramraj S, Benbrook DM, Bieniasz M, Wang L, Pathuri G, Isingizwe ZR, Kennedy AL, Zhao YD, Lightfoot S, Hunsucker LA, Gunderson CC. Potential and mechanism of mebendazole for treatment and maintenance of ovarian cancer. *Gynecol Oncol.* 2021;160:302-311.